Optical Evidence for the Metallization of Xenon at 132(5) GPa

Kenneth A. Goettel, Jon H. Eggert, and Isaac F. Silvera
Lyman Laboratory of Physics, Harvard University, Cambridge, Masschusetts 02138

William C. Moss
Lawrence Livermore National Laboratory, University of California, Livermore, California 94550
(Received 2 May 1988)

We have compressed xenon in a diamond-anvil cell to approximately 200 GPa. The metallization of xenon by band-gap closure was investigated by obtaining optical data in both the metallic and insulating states. In the metallic state, we determined the pressure dependence of the plasma frequency from absorption data fitted with a free-electron model. In the insulating state, we determined the pressure dependence of the band gap from absorption data fitted with an indirect-band-gap model. Our optical data indicate that the insulator-to-metal transition in xenon occurs at 132(5) GPa.

PACS numbers: 71.30.+h, 78.30.Er, 78.40.Kc

The metallization of insulators by band-gap closure at high pressure has been of interest for more than sixty years.[1] Rare-gas solids, the simplest atomic solids, are particularly accessible to theoretical investigation. Xenon, the rare gas having the lowest predicted metallization pressure, is of particular interest experimentally. In this paper we present the first optical data demonstrating the insulator-to-metal transition in xenon.

The metallization of xenon has been a controversial subject for the past decade. Band-structure calculations for fcc and bcc xenon[2-8] have predicted metallization pressures ranging from 82 to 200 GPa. Metallization of xenon was reported in diamond-indentor experiments by Nelson and Ruoff[9] at 33 GPa (later revised to greater than 100 GPa[10]) and by Yakovlev, Timofeev, and Vinogradov[11] at an unspecified pressure. Subsequent diamond-anvil cell measurements of the energy-band gap[12-15] showed that the gap remains in the ultraviolet to 55 GPa. Extrapolation of these band-gap measurements suggested metallization at 200 GPa or higher.[13] Recently, Jephcoat *et al.*[16] obtained x-ray data on xenon to 137 GPa in a diamond-anvil cell; there was no visual evidence for band-gap closure, although the molar volume was close to that predicted at metallization by the Herzfeld criterion.[1]

The objective of the present experiment was to improve understanding of xenon at high pressure by obtaining optical data in the metallic as well as in the insulating state. The experimental parameters (including rhenium gasket material, diamond design, and sample configuration) were a direct application of the principles for maximizing the pressure obtainable in a soft-sample experiment given by Moss *et al.*[17] and Moss and Goettel.[18,19] In the present experiment, we applied techniques developed at Harvard and by the references cited above.[17-19]

We loaded high-purity xenon in a slightly modified Mao-Bell–type diamond-anvil cell[20] with type-Ia diamonds, using the cryogenic loading scheme described by Silvera and Wijngaarden,[21] although the cryostat was a liquid-nitrogen–cooled box. Upon warming to room temperature, the xenon was at approximately 200 GPa, due to overestimation of the force required to produce a given sample pressure. The xenon sample had an area of 190 μm^2 measured in transmitted light and a thickness of 10(3) μm, estimated from finite-element modeling and previous experiments.[17-19,22]

Optical data were initially obtained at 200 GPa. Subsequently, the pressure was gradually lowered and optical data were acquired down to 107 GPa. Pressures were measured by the ruby-fluorescence method using the time-resolved detection method developed by Eggert, Goettel, and Silvera.[23] Ruby pressure measurements were made in the xenon at 158 GPa and below, using the quasihydrostatic pressure scale.[24] At higher pressures, ruby measurements could not be made in the xenon because of diminished ruby-fluorescence intensity and absorption in the xenon. To determine xenon pressures above 158 GPa, radial pressure profiles were measured across the gasket surface (up to 164 GPa using the nonhydrostatic ruby scale[25]) and extrapolated to the xenon sample region. The validity of this extrapolation method was confirmed by the agreement between extrapolated pressure estimates and direct pressure measurements in the xenon sample at 158 GPa and below.

Pressure measurements in the xenon between 107 and 142 GPa indicated that pressure gradients across the xenon sample ranged from 0.5 to 1.0 GPa/μm. At 200 GPa, the radial pressure profiles suggested that the pressure gradient within the xenon sample may have been as much as twice as large. The quasihydrostatic behavior of xenon noted at lower pressures[16] may be due in part to shear between layers in the mixed-phase regime. Above 75 GPa, in the hcp phase, xenon should exhibit the usual increase in yield strength with increasing pressure.

Optical measurements were made using various sources: a quartz-tungsten-halogen lamp and argon-

ion, neodymium-doped-yttrium-aluminum-garnet, (Nd-YAlG), F-center and CO_2 lasers. Several detectors were used: a silicon diode array, a germanium photodiode, and laser photodetectors. All data other than the laser data points were taken with a grating spectrometer.

The results of our absorption and reflectivity measurements are shown in Fig. 1. Infrared absorption data were collected from the entire xenon sample. Visible absorption data were collected with a spatial filter which limited the sampling area to an 8 μm diameter. Absorption coefficients were corrected for reflections from the diamond interfaces and for the difference in area between the xenon and a 275-μm^2 reference pinhole. Ruby constituted only about 5% of the sample area and thus did not contribute significantly to the observed absorption. Reflectivity data, collected at 200 GPa with a 4-μm-diam sampling area, were referenced to the second diamond-air interface of a reference diamond and thus were corrected for air-diamond reflection and diamond absorption. Nonhydrostatic stress in the xenon sample could affect the data[26]; absorption and reflectivity data obtained at 200 GPa with a 4-μm-diam sampling area showed that effects due to the pressure gradient across the xenon sample were significant, but small relative to the differences in absorption at successive pressures [Fig. 1(b)].

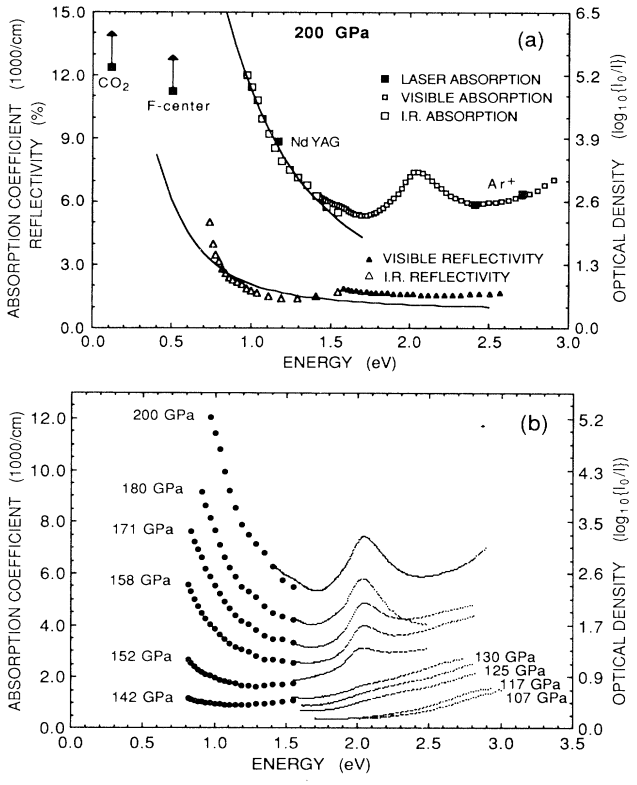

FIG. 1. (a) Absorption and reflectivity of metallic xenon at 200 GPa. Note the different vertical scales for the absorption coefficient and reflectivity data. The two drawn lines were calculated from the fit to the infrared absorption data as described in the text. The CO_2 and F-center laser absorption points are detection-limited lower bounds. (b) Absorption data for xenon in the metallic and insulating states.

Although diamond at 1 bar is very transparent at the wavelengths of our measurements, pressure-induced changes in diamond absorption could conceivably contribute to the observed spectra. If diamond became absorbing at high pressure, however, we would have observed this absorption in the reflection spectra and this was not the case. We are confident, therefore, that the main features observed in the absorption spectra are due to the xenon.

The F-center and CO_2 laser data [Fig. 1(a)] were obtained at 200 GPa with the same technique as the argon-ion and Nd-YAlG laser data. The concordance of the argon-ion and Nd-YAlG laser data with the diode-array and germanium-detector data substantiates the validity of our laser absorption measurement techniques. Using the F-center and CO_2 lasers, no light transmitted through the xenon was detectable. The lower bounds for these data [Fig. 1(a)] are conservative and are based on confidence tests of our measurement techniques, including detector sensitivities, noise levels, and spatial alignments.

The sharp rise in absorption and reflectivity below about 1.5 eV (Fig. 1) is characteristic of a classical free-electron metal near the plasma frequency. We fitted the real and imaginary parts of the complex dielectric function ($\epsilon=\epsilon_1+i\epsilon_2$) to the absorption data using a Drude free-electron model, including the scattering relaxation time approximation[27]:

$$\epsilon_1=n^2-k^2=\epsilon_{IB}-\frac{\omega_p^2\tau^2}{1+\omega^2\tau^2},\quad \epsilon_2=2nk=\frac{\omega_p^2\tau}{\omega(1+\omega^2\tau^2)}.$$

The absorption coefficient (α) and the reflectivity (R) are given by $\alpha=(2\omega/c)k$ and $R=|(N-2.4)/(N+2.4)|^2$. Here, $N=n+ik$, is the complex index of refraction, 2.4 is the index of refraction of diamond, ω_p is the plasma frequency, τ is the relaxation time, and ϵ_{IB} is the real part of the dielectric constant due to higher-energy interband transitions. Based on our visible reflectivity data at 200 GPa and the data of Itie and Le Toullec,[28] we chose a constant value of $\epsilon_{IB}=4$ (i.e., $n_{Xe}=2$) for the pressure range of our data in the metallic state.

Fits were obtained for absorption data between 152 and 200 GPa [Table I, Fig. 1(a)]. The lower bounds from the CO_2 and F-center laser measurements [Fig. 1(a)] are consistent with the high absorption coefficients calculated at these energies. The reflectivity at 200 GPa, calculated from our fit of the absorption data with no additional adjustable parameters, agrees qualitatively with the observed rise in reflectivity. Near the plasma frequency, the calculated absorption and reflectivity agree

TABLE I. Compilation of the pressure and volume points at which optical measurements were made, along with values for ω_p, $\omega_p\tau$, and E_{gap}.

Pressure (GPa)	Volume (cm^3/mol)	ω_p (eV)	$\omega_p\tau$	E_{gap} (eV)
200(20)	9.40(30)	0.982(21)	1.84(15)	···
180(15)	9.72(25)	0.803(18)	1.33(16)	···
171(5)	9.88(9)	0.692(11)	1.11(13)	···
158(5)	10.12(10)	0.572(8)	0.79(13)	···
152(5)	10.24(10)	0.416(8)	0.30(8)	···
142(5)	10.46(11)	···	···	···
130(5)	10.75(12)	···	···	0.063(21)
125(5)	10.88(13)	···	···	0.325(20)
117(5)	11.10(15)	···	···	1.201(14)
107(5)	11.41(16)	···	···	1.212(21)

well with our data. We attribute the divergence between the fits and the data at higher energies to interband transition structure which was not considered in our model.

The high-pressure absorption and reflectivity data (Fig. 1) suggest that the xenon is metallic. Assuming quadratic electron energy-band shapes and a linear band shift with volume (for small volume changes), ω_p will shift as $(\Delta V)^{3/4}$, where ΔV is the molar volume difference from the volume at metallization. In Fig. 2(a) we plot $\omega_p^{4/3}$ vs V; a linear χ^2 fit yields a molar volume of 10.65(18) cm^3/mol, corresponding to a pressure of 134(7) GPa, at metallization (i.e., ω_p goes to zero). We used a Birch-Murnaghan equation of state for xenon fitted to the data given by Jephcoat *et al.*[16] with 7.32 GPa for the bulk modulus, 4.47 for the pressure derivative of the bulk modulus, and a zero-pressure volume of 34.7 cm^3/mol.[3]

The interpretation of our data on xenon in the metallic state is substantiated by our absorption measurements in the insulating state. Our absorption spectra for pressures below 142 GPa display a rise in absorption with increasing energy [Fig. 1(b)] which we interpret as the absorption edge. The magnitude of this absorption rise is consistent with that observed at lower pressures for absorption-edge measurements in the ultraviolet.[12-15] For indirect-band-gap materials, such as xenon,[2] absorption is expected to be quadratic in energy above the band-gap energy.[29] The band gaps determined from extrapolation of our visible absorption data are given in Table I. Assuming again that the bands shift linearly with volume, a χ^2 fit to our data [Fig. 2(a)] yields 10.73(10) cm^3/mol, 131(4) GPa, at metallization (i.e., the band gap goes to zero). Including possible systematic errors in the zero absorption background level, we obtain 131(10) GPa for the metallization pressure from these absorption measurements.

We interpret the peak in absorption at 2.05 eV (Fig. 1) as an unidentified interband transition. A similar absorption feature near 2 eV has also been observed in other xenon experiments.[30] A possible explanation is that this transition is due to electrons in the conduction band or holes in the valence band. In either case this absorption feature would be a signature of metallization. The integrated absorption of such a feature would be proportional to the number of free electrons and thus proportional to $(\Delta V)^{3/2}$, assuming linear band shifts with volume. In Fig. 2(b), we plot the integrated absorption to the $\frac{2}{3}$ power versus molar volume. A linear χ^2 fit indicates that the line strength goes to zero at 10.72(13) cm^3/mol, 131(6) GPa, in excellent agreement with the metallization pressures determined above from the plasma frequency and the absorption edge. Confirmation of this interpretation requires detailed band-structure calculations.

We have interpreted our visible and infrared optical data for xenon to obtain three independent determinations of the insulator-to-metal transition in xenon. Combining our three determinations we obtain metallization at 10.70(12) cm^3/mol, 132(5) GPa.

The apparent discrepancy between our determination

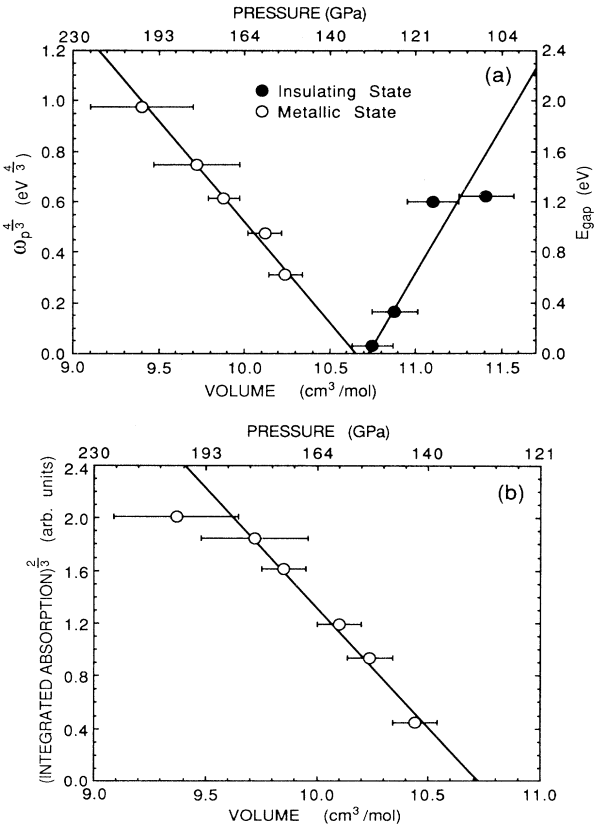

FIG. 2. (a) Linear χ^2 fits of the volume dependence of $\omega_p^{4/3}$ in the metallic state and the volume dependence of the band gap in the insulating state. (b) Linear χ^2 fit of the integrated absorption of the absorption feature at 2.05 eV to the $\frac{2}{3}$ power vs molar volume.

of metallization at 132(5) GPa and the absence of visual evidence for band-gap closure to 137 GPa by Jephcoat *et al.*[16] is understandable. The absorption edge in xenon, from our data between 107 and 130 GPa and earlier measurements at low pressure,[12-15] is broad, weak, and difficult to detect visually. Furthermore, xenon in the metallic state transmits some light in the visible (particularly at pressures just above metallization) and there is not a large visual change near the pressure of metallization.

Finally, we note that our determination of the molar volume of xenon at metallization , 10.70(12) cm^3/mol, is slightly larger than that predicted by the Herzfeld criterion,[1] 10.2 cm^3/mol.

We thank R. Yandrofski for contributions to the early stages of this experiment. Numerous discussions with J. Brisson, H. Lorenzana, J. Mester, and B. Morris are acknowledged. We thank C. Lobb, M. Tinkham, W. Paul, and F. Pipkin for their generous loan of optical equipment, as well as H. Cheong, C. Johnson, and P. Zhao for assistance with some of the infrared measurements. We thank John Nuckolls, Director, Lawrence Livermore National Laboratory, for support and encouragement. This work received support from Harvard Materials Research Laboratory NSF Grant No. DMR-14003 and NASA Grant No. NAGW-657. W. Moss's work was performed under the auspices of the U.S. Department of Energy at Lawrence Livermore National Laboratory under Contract No. W-7405-Eng-48.

[1]K. F. Herzfeld, Phys. Rev. **29**, 701 (1927).

[2]M. Ross, J. Chem. Phys. **56**, 4651 (1972).

[3]M. Ross and A. K. McMahan, Phys. Rev. B **21**, 1658 (1980).

[4]A. K. Ray, S. B. Trickey, R. S. Weidman, and A. B. Kunz, Phys. Rev. Lett. **45**, 933 (1980).

[5]M. Ross and A. K. McMahan, in *Physics of Solids under Pressure,* edited by J. S. Schilling and R. N. Shelton (North-Holland, New York, 1981), p. 161.

[6]Yu. Kh. Vekilov and L. Z. Kimlat, Dokl. Akad. Nauk. SSSR **257**, 590 (1981) [Sov. Phys. Dokl. **28**, 317 (1981)].

[7]J. Hama and S. Matsui, Solid State Commun. **37**, 889 (1981).

[8]A. K. Ray, S. B. Trickey, and A. B. Kunz, Solid State Commun. **41**, 351 (1982).

[9]D. A. Nelson, Jr. and A. L. Ruoff, Phys. Rev. Lett. **42**, 383 (1979).

[10]K. S. Chan, T. L. Huang, T. A. Grzybowski, T. J. Whetten, and A. L. Ruoff, Phys. Rev. B **26**, 7116 (1982).

[11]E. N. Yakovlev, Yu. A. Timofeev, and B. V. Vinogradov, Pis'ma Zh. Eksp. Teor. Fiz. **29**, 400 (1979) [JETP Lett. **29**, 362 (1979)].

[12]K. Syassen, Phys. Rev. B **25**, 6548 (1982).

[13]K. Asaumi, T. Mori, and Y. Kondo, Phys. Rev. Lett. **49**, 837 (1982).

[14]I. Makarenko, F. Weill, J. P. Itie, and J. M. Besson, Phys. Rev. B **26**, 7113 (1982).

[15]J. M. Besson, J. P. Itie, G. Weill, and I. Makarenko, J. Phys. (Paris), Lett. **43**, L401 (1982).

[16]A. P. Jephcoat, H.-k. Mao, L. W. Finger, D. E. Cox, R. J. Hemley, and C.-s. Zha, Phys. Rev. Lett. **59**, 2670 (1987).

[17]W. C. Moss, J. O. Hallquist, R. Reichlin, K. A. Goettel, and S. Martin, Appl. Phys. Lett. **48**, 1258 (1986).

[18]W. C. Moss and K. A. Goettel, Appl. Phys. Lett. **50**, 25 (1987).

[19]W. C. Moss and K. A. Goettel, J. Appl. Phys. **61**, 4951 (1987).

[20]H. K. Mao and P. M. Bell, Carnegie Inst. Washington, Yearb. **77**, 904 (1978).

[21]I. F. Silvera and R. J. Wijngaarden, Rev. Sci. Instrum. **56**, 121 (1985).

[22]K. A. Goettel, H.-k. Mao, and P. M. Bell, Rev. Sci. Instrum. **56**, 1420 (1985).

[23]J. H. Eggert, K. A. Goettel, and I. F. Silvera, Appl. Phys. Lett. **19**, 2489 (1988).

[24]H. K. Mao, J. Xu, and P. M. Bell, J. Geophys. Res. **91**, 4673 (1986).

[25]P. M. Bell, H. K. Mao, and J. A. Xu, in *Shock Waves in Condensed Matter,* edited by Y. M. Gupta (Plenum, New York, 1986), p. 125.

[26]J. P. Itie, A. Polian, and J. M. Besson, Phys. Rev. B **30**, 2309 (1984).

[27]J. M. Ziman, *Principles of the Theory of Solids* (Cambridge Univ. Press, Cambridge, 1972), Chap. 8.

[28]J. P. Itie and R. Le Toullec, J. Phys. (Paris), Colloq. **45**, C8-8 (1984).

[29]O. Madelung, *Introduction to Solid State Theory* (Springer-Verlag, Berlin, 1978).

[30]R. Reichlin and M. Ross, private communication.